

New quantum state formed by highly concentrated protons in superconducting palladium hydride

Ryoma Kato,¹ Ten-ichiro Yoshida,¹ Riku Iimori,² Tai Zizhou,¹ Masanobu Shiga,¹ Yuji Inagaki,³ Takashi Kimura,² Koichiro Ienaga,⁴ and Tatsuya Kawae^{1,*}

¹*Department of Applied Quantum Physics,
Kyushu University, Motooka, Fukuoka 819-0395, Japan*

²*Department of Physics, Kyushu University,
Motooka, Fukuoka 819-0395, Japan*

³*Institute for the Advancement of Higher Education,
Okayama University of Science, Ridaicho,
Kita-ku, Okayama 700-0005, Japan*

⁴*Graduate School of Sciences and Technology for Innovation,
Yamaguchi University, Ube, Yamaguchi, 755-8611, Japan*

Abstract

Hydrogen exhibits quantum phenomena, such as tunneling in materials. According to theory, the quantum properties of hydrogen change significantly in superconductors due to the emergence of an energy gap on the Fermi surface, which reduces the interaction between hydrogen nucleus (i.e., proton) and conduction electrons. This reduction is predicted to enhance the tunneling probability of protons. Here, we report the double transitions of the electrical resistivity in high-quality palladium hydride (PdH_x) and deuteride (PdD_x) prepared by low-temperature absorption below $T = 180$ K. After a sharp drop in the resistivity at $T \sim 2$ K owing to the superconducting transition of PdH(D)_x , a large residual resistivity remained. Additionally, the resistivity dropped to zero below $T = 1$ K. The experimental results suggest that the quantum tunneling of highly concentrated protons (deuterons) in the superconducting state is responsible for the observed features: the residual resistivity arises from the weakening of the global coherence of superconductivity owing to the tunneling motion of protons (deuterons), while the zero resistivity is caused by long-range ordering of the protons (deuterons). This system offers a new platform for investigating the quantum many-body properties of tunneling particles.

*Electronic address: t.kawae.122@m.kyushu-u.ac.jp

I. INTRODUCTION

Hydrogen (H), with the smallest atomic mass, exhibits various quantum phenomena in materials at low temperatures. In transition metals, where H atoms occupy interstitial sites, they migrate by quantum tunneling [1–4] in a sea of conduction electrons at low temperatures, as shown in Fig. 1(a) [5–7]. Theories indicate that this situation varies significantly in the superconducting state [8–13]. An energy gap appears on the Fermi surface, which suppresses the interaction between hydrogen nucleus (i.e., proton) and conduction electrons, as illustrated in Figs. 1(b) and 1(c), and then influences the quantum behavior of the H atoms. For example, the tunneling probability of a proton is predicted to increase exponentially with decreasing temperature. However, experimentally, the variation in the tunneling features of H at the interstitial site due to the superconducting transition has not been revealed. Notably, the tunneling diffusion of muons with a mass of approximately 1/9 that of a proton has been confirmed to increase markedly after the superconducting transition [14], which is in good agreement with the theoretical prediction.

Palladium-hydride (PdH_x) is suitable not only for studying the role of H in the occurrence of superconductivity in hydride systems but also for exploring the quantum behaviors of highly concentrated H in superconductors. This is because the superconducting transition of PdHx occurs for the H concentration $x \gtrsim 0.72$ under ambient pressure [15, 16]. Moreover, the transition temperature T_c increases with H concentration¹⁷⁾ and reaches T_c of 9 K for a stoichiometric concentration of $x = 1$ [18, 19]. This facilitates various experimental investigations, in contrast to room-temperature superconductors in H-rich materials discovered at extremely high pressures [20–22]. However, the superconducting properties of PdH_x have not been sufficiently investigated so far owing to the low quality of PdH_x samples, which results in a broadening of the superconducting transition.

We successfully prepared a high-quality sample of PdH_x using a low-temperature H absorption method, in which H atoms were loaded into Pd under an H_2 atmosphere below $T = 200$ K [19, 23]. Subsequently, the PdH_x sample was cooled to a low temperature for the measurements without H desorption. For PdH_x powders with diameters of 1–2 μm , the superconducting volume fraction reached ~ 1 , indicating that samples with a uniform H concentration can be obtained [19, 23] Using this method, we studied the temperature dependence of the resistivity of the PdH_x films [24, 25]. By loading H atoms in a Pd film

with a thickness of 100 nm for approximately 20 days, a PdH_x film with a superconducting transition width below 0.1 K (where $T_c \sim 1.1$ K) was achieved, which was considerably narrower than that of the previous measurements. However, a residual resistance of unknown origin remained.

In this paper, we report the discovery of double transitions in the resistivities of PdH_x and PdD_x films. As in our previous studies, the residual resistivity appears below the superconducting transition. In addition, zero resistivity is observed below the second transition in the lowest-temperature region. The observed features can be interpreted as tunneling motion and the ordering of highly concentrated protons or deuterons in the superconducting state.

II. EXPERIMENTAL

We studied the electrical resistivity of two types of Pd films with a thickness of 100 nm, which is considerably larger than the coherence length of superconducting PdH_x [16, 23]. One is a Pd film deposited on an Au electrode, which enables the absorption of H atoms in the Pd film without obstructing the electrodes. The other is that Cu electrodes are deposited on the Pd film, which was prepared for comparison with the Au electrode results. The detail of the sample synthesis is presented in Appendix.

The resistivity measurements were conducted in the same manner as in the previous measurements [25]. The Pd film was mounted on a Cu plate installed in a homemade ³He insert that was attached to a Quantum Design MPMS SQUID magnetometer [26]. The resistance of the film was measured by a four-wire method using an LR700 AC resistance bridge down to a temperature of ~ 0.6 K, from which the resistivity was estimated. The RuO₂ thermometer was attached to the Cu plate [25]. A magnetic field was applied parallel to the PdH_x film along the current direction. It should be noted that the field deviates from the parallel direction because a thin Cu plate is used as the sample holder, which deforms easily during the mounting of the holder onto the ³He insert. The experimental procedure is detailed in Appendix.

III. RESULTS

A. Temperature dependence of resistivity in PdH_x films

In the previous measurements, the electrodes were attached to a Pd film using silver (Ag) paste [24, 25]. However, in this setup, H absorption may be prevented by the electrode, resulting in H deficiency. Consequently, residual resistivity could appear below the superconducting transition temperature. Therefore, in the present study, we prepared new Pd films with a thickness of 100 nm and width of 100 μm on Au electrodes (Fig. A-1(a)), which enabled the absorption of H atoms in the Pd film without obstruction by the electrodes. Figure 2(a) shows the temperature dependence of resistivity below 5 K for the PdH_x film, where H absorption was performed at $T = 150$ K.

The resistivity is constant above the superconducting transition temperature, dropping sharply below $T_{c1} = 2.14$ K; the transition finishes at 2.0 K, reflecting a uniform H distribution in the film. The H concentration is estimated to be $x = 0.865$ from the transition temperature $T_{c1} = 2.14$ K [17]. Despite the sharp drop, a large residual resistivity remains, exhibiting a gradual decrease with decreasing the temperature, as shown in the inset of Fig. 2(a). These features are qualitatively the same as those in the previous measurements with electrodes on a Pd film [24, 25]. Notably, the second transition with a step drop in resistivity occurs at $T_{c2} = 0.78$ K, resulting in zero resistivity. It is also significant that the ratio of residual resistivity below T_{c1} to the resistivity in the normal state is much larger than that of the previous measurements with electrodes on the Pd film. This indicates that the residual resistivity is not caused by H deficiency due to the electrodes covering the Pd film.

To clarify the origin of the residual resistivity and second transition, we performed two measurements, varying (i) the H concentration and (ii) the size of the film (details of measurement (ii) are described in Appendix “Resistivity measurements in 10 μm wide film”). To increase the H concentration of the film, the temperature of the PdH_{0.865} film was raised to $T = 150$ K, and the film was exposed to an H₂ gas atmosphere (the procedure is outlined in Appendix “Procedure of hydrogen absorption into Pd film”). After reabsorption, the temperature dependence of the resistivity was measured again, as depicted by the red plots in Fig. 2(b). The normal resistivity before the superconducting transition decreases

owing to the increase in H concentration [27]. Moreover, the two transition temperatures are increased to $T_{c1} = 2.31$ K, corresponding to $x = 0.870$, and $T_{c2} = 0.86$ K. Subsequently, the H concentration was decreased by increasing the temperature to $T = 180$ K to desorb H from the film, as shown by the green plots in Fig. 2(b). The superconducting transition temperature decreases to $T_{c1} = 1.28$ K, corresponding to $x = 0.834$, whereas the second transition is invisible. The H concentration of the film was increased again by reabsorbing H into the film, raising the two transition temperatures to $T_{c1} = 1.85$ K at $x = 0.855$ and $T_{c2} = 0.69$ K, as depicted by black plots in Fig. 2(b).

The concentration dependences of T_{c1} and T_{c2} are plotted in Fig. 2(d). Through H absorption and desorption, T_{c2} appears to change almost linearly as a function of the H concentration. T_{c2} at $x = 0.834$ is not visible because it is estimated to be lower than the minimum temperature in the experiment. Evidently, the slope of T_{c2} is different from that of T_{c1} . Additionally, the magnitude of the residual resistivity above T_{c2} is approximately the same for all concentrations, as shown in Fig. 2(c), in contrast to the marked variation in the resistivity in the normal region, which depends remarkably on the H concentration [27]. These results strongly suggest that the origin of T_{c2} is not caused by H deficiency.

Similar characteristics are observed in the PdH_x film with a width of $10 \mu\text{m}$, which is one-tenth the size of the current film (Fig. A-3). This indicates that the residual resistivity and the second transition do not depend on the sample size.

We examined the influence of Au electrodes covered with a Pd film. Since Au can form an Au-Pd alloy [28, 29], it might affect the superconducting transition of the Pd film. To assess this possibility, we measured the resistivity of a PdH_x film with a different electrode structure, in which Cu electrodes were deposited on the Pd film illustrated in Fig. A-1(b), meaning that the electrodes were not covered by the Pd film. Details of this measurement are given in Appendix “Resistivity in Pd film with Cu electrodes”. The qualitative features are consistent with those obtained for the Au electrodes. These results demonstrate that the emergence of the residual resistivity and the second transition do not originate from the influence of the Au electrodes but from the intrinsic features of superconducting PdH_x .

B. Magnetic field dependence of superconducting transition in PdH_x film

Figures 3(a) and 3(b) show the magnetic field dependence of the resistivity around T_{c1} and T_{c2} , respectively, in the PdH_{0.870} film. As the magnetic field increases, the superconducting transition at T_{c1} is suppressed with broadening the transition curve, as in the case of conventional superconducting transitions. In contrast, although T_{c2} is also suppressed, the sharp drop in resistivity is maintained up to $H = 800$ Oe, which is the maximum field at which T_{c2} can be observed. For instance, at $H = 0$ Oe, the resistivity starts to deviate at 0.86 K and decreases to zero at 0.83 K, while at $H = 800$ Oe, these values are at 0.59 K and 0.56 K, respectively. These characteristics are clearly illustrated in the phase diagram of T_{c1} and T_{c2} in Fig. 3(d), where no broadening of T_{c2} is observed up to $H = 800$ Oe. These results suggest that the transition at T_{c2} does not originate from the superconducting transition of PdH_x.

Figure 3(c) plots the field dependence of the resistivity as the magnetic field increases at $T = 0.6$ K in PdH_{0.870} film. As the magnetic field increases, the resistivity rises steeply at $H = 770$ Oe and reaches the value of the residual resistivity at $H = 800$ Oe, as shown in the inset. Subsequently, the resistivity is constant up to ~ 2500 Oe, which is followed by a gradual increase and rises sharply at approximately $H = 2700$ Oe. This value is in reasonable agreement with the upper critical field observed in the magnetization curve of PdH_{0.870}, where the measurements were performed in the powder sample with a diameter of $1\sim 2$ μm [16]. However, a transition at T_{c2} cannot be observed in the magnetization curve. This also supports that the transition at T_{c2} does not originate from the superconducting transition of PdH_x.

C. Superconducting transition in PdD_x film

Finally, we present the resistivity of a palladium deuteride (PdD_x) film, where the Pd film has a thickness of 100 nm and a width of 100 μm , deposited on the Au electrodes (Fig. A-1(a)). The temperature and magnetic dependences of the resistivity is shown in Figs. 4(a) and 4(b), respectively. The overall features are similar to those observed in the PdH_x measurements. The resistivity decreases sharply at $T_{c1} = 1.47$ K owing to the superconducting transition, from which the deuterium concentration is estimated to be x

$= 0.795$ [17]. A large residual resistivity remains below T_{c1} , and a steep drop in resistivity, attributed to the second transition, occurs at $T_{c2} \sim 0.6$ K. The magnitude of the residual resistivity above T_{c2} is approximately the same as that in the PdH_x film with the same sample size shown in Figs. 2(a)-2(c), despite the fact that the mass of deuterium is twice that of a proton. As the magnetic field increases, the superconducting transition at T_{c1} is suppressed with broadening the transition curve.

However, a close examination of the temperature dependence demonstrates a clear difference between the PdH_x and PdD_x results. In the $\text{PdD}_{0.795}$ film, a rectangular-shaped anomaly appears between $T = 0.95$ and 1.2 K, as presented in the inset of Fig. 4(a). As the magnetic field increases, this anomaly shifts to lower temperatures (Fig. 4(c)), where T_{c1} decreases with the broadening of the resistivity curve, as shown in Fig. 4(b). Since a rectangular anomaly is not detected in the PdH_x film, it is reasonable to consider that an isotope effect contributes to the properties of the residual-resistivity state in superconducting PdD_x [30].

IV. DISCUSSION

As described above, the residual resistivity in PdH(D)_x films cannot be explained by H deficiency or the influence of the electrodes, indicating that the emergence of the residual resistivity followed by the second transition is an intrinsic feature of a high-quality PdH(D)_x film. These results strongly suggest that protons (deuterons) immersed in the superconducting state play a pivotal role in the observed features. Similar behaviors, that is, residual resistivity followed by a zero-resistivity transition, have been observed in several systems, for example, vortex liquid-lattice transition in a superconductor [31, 32], and charge density wave (CDW) coexisting with superconductivity [33], in which the resistive state exists in the superconducting state. In the vortex system, the motion of the vortices disrupts the global coherence of superconductivity, generating resistivity in the vortex liquid state, whereas freezing the motion leads to zero resistivity. Notably, a sharp anomaly in resistivity emerges at the vortex liquid-lattice transition [32].

Similarly, the liquid-like tunneling motion of protons is expected to disrupt the global coherence of superconductivity. According to theories [9, 34, 35], the energy dissipation of tunneling protons is inevitable due to the interaction with the electron and lattice sys-

tems, causing phase fluctuation of the superconducting wave function. Consequently, the global coherence of the superconducting state is disrupted, leading to residual resistivity. Conversely, when protons or deuterons order, the effective mass of the tunneling particle increases, dramatically decreasing the tunneling probability. This results in the observation of zero resistivity. This scenario is consistent with the fact that the anomaly at T_{c2} cannot be observed in the magnetization measurements, which are sensitive to vortex penetration.

The residual resistivity of the PdH_x films with Au electrodes is considerably larger than that of the Cu and Ag electrodes presented in our previous paper [25]. This difference could be attributed to variations in tunneling probability, which are influenced by the energy difference between potential wells at the tunneling site, as illustrated in Fig. 1(a) [9]. Attaching electrodes after film deposition can degrade the homogeneity of the Pd film. This degradation increases the potential difference ($\Delta\varepsilon$) between the two wells for H tunneling, thereby suppressing tunneling probability by widening the potential difference at the tunneling sites [9]. Accordingly, the residual resistivity is lower for Cu and Ag electrodes than Au electrodes.

Finally, we consider the nature of the ordering below T_{c2} . PdH_x system is known to undergo a glass-like transition at approximately 50 K [36]. Below T_{c1} , the protons move in a liquid-like manner owing to an increase in the tunneling probability, which should lead to ordering at lower temperatures. Therefore, one possibility is a structural ordering that stabilizes the proton or deuteron positions. Indeed, the lack of a clear correlation between T_{c1} and T_{c2} across different PdH_x films, as shown in Fig. 2(d), supports this idea. However, simple structural ordering cannot explain the rectangular anomaly in the resistivity of PdD_x .

Another possibility is the magnetic ordering or condensation of protons and deuterons. The emergence of the rectangular anomaly, detected exclusively in the PdD_x film, indicates that the statistical differences arising from the nuclear spin degree of freedom ($I = 1/2$ for protons, $I = 1$ for deuterons) influence the tunneling behavior of PdH_x and PdD_x . This effect becomes particularly significant in the highly concentrated H or D regime, where superconductivity occurs for $x \gtrsim 0.75$. Since nuclear spin contributions typically manifest at temperatures well below $T = 1$ K [37], the emergence of the rectangular anomaly around $T = 1$ K suggests that nuclear contributions are enhanced by quantum many-body interactions between protons (or deuterons) and the electron and/or lattice systems. These interactions may influence the ordering process as well as the tunneling behavior. Clearly, further exper-

imental and theoretical studies are needed to gain a deeper understanding of the tunneling dynamics and ordering mechanisms.

V. CONCLUSION

We observed double transitions in the electrical resistivities of the PdH(D)_x films. Despite a sharp superconducting transition at T_{c1} , a large residual resistivity persists below T_{c1} , which then drops to zero at T_{c2} . The experimental results are explained by assuming that the tunneling probability of protons (deuterons) is enhanced by the formation of a superconducting gap, as suggested by theories [8–13]. The tunneling motion of protons (deuterons) disrupts the global coherence of superconductivity, causing residual resistivity. An ordering of the tunneling motion at T_{c2} increases the effective mass, suppressing the tunneling probability and leading to zero resistivity. These findings suggest that tunneling protons (deuterons) in superconductors form novel quantum states, opening a pathway for studying the quantum many-body properties of tunneling particles.

VI. ACKNOWLEDGMENTS

We specially thank Profs. Matsumoto, Shirahama and Maruyama for fruitful discussion. We also thank Professor Yamamuro for providing information about the low-temperature H absorption into Pd. We also thank Mrs. Hasuo and Yamaguchi for their technical help. This work was supported by JSPS KAKENHI Grant Numbers JP23K17763 and JP21H01605, Nippon Sheet Glass Foundation for Materials Science and Engineering, and Murata Science Foundation.

VII. APPENDIX

A. Synthesis of Pd film

We studied the electrical resistivity of two types of Pd films with a thickness of 100 nm, which is considerably larger than the coherence length of superconducting PdH_x [16, 23]. One is a Pd film deposited on an Au electrode, which enables the absorption of H atoms in the Pd film without obstructing the electrodes, as shown in Fig. A-1(a). Au electrodes with

thickness of 20 nm and width of 50 μm were prepared on a SiO_2/Si substrate by electron beam evaporation. To adhere the Au electrodes to the substrate firmly, a 5-nm Ti layer was deposited below the Au electrodes. Subsequently, a Pd film with a thickness of 100 nm and width of 100 μm was deposited on the substrate with Au electrodes by magnetron sputtering under a base pressure of 5.5×10^{-6} Pa. The distance between the two voltage electrodes was 300 μm . In addition, a Pd film with a thickness of 100 nm and a width of 10 μm , deposited on Au electrodes, was prepared to reveal the influence of the film size.

The other film with Cu electrodes is shown in Fig. A-1(b). This sample was prepared for comparison with the Au electrode results. First, a Pd film with a thickness of 100 nm and a width of 100 μm was deposited on a SiO_2/Si substrate by magnetron sputtering under a base pressure of 5.5×10^{-6} Pa. Subsequently, Cu electrodes with a thickness of 100 nm and width of 50 μm were deposited on the Pd film by thermal evaporation. The distance between the two electrodes was 300 μm .

B. Low-temperature hydrogen absorption method

H absorption was performed at temperatures below $T = 180$ K. As shown in Fig. A-2, the H concentration x in Pd increases as the temperature decreases. For example, when metallic Pd is exposed to an H_2 pressure of 0.1 MPa at $T = 200$ K, the H concentration in Pd reaches approximately $x \sim 0.8$, which exceeds the critical concentration required for superconductivity in PdH_x . Using this low-temperature H absorption method, we conducted H charging in Pd metal and observed the superconducting transition through in-situ magnetization or resistivity measurements down to $T \sim 0.6$ K. In this study, we prepared PdH(D)_x films by varying the absorption temperature; the H_2 (D_2) pressure was ~ 0.25 MPa.

C. Procedure of hydrogen absorption into Pd film

The H absorption into the Pd film was conducted using the following procedure: Before cooling the sample for H absorption, several activation processes were performed at $T = 320$ K by exposing the film to H_2 gas and evacuating it to remove surface contaminants and rearrange the surface structure to increase the H-absorption speed. After activation, the Pd film was cooled to $T = 180$ K, and H_2 gas at the pressure of ~ 0.25 MPa was introduced

into the experimental chamber. With increasing H content in the film, the resistance varies remarkably [25, 27, 38, 39].

The resistance variation approaches constant, demonstrating that the H content in the film is close to the equilibrium concentration at ~ 0.25 MPa and 180 K. Thereafter, the temperature was decreased to 170 K for further H absorption. We repeated the above procedure in increments of 10 K. After H absorption at $T = 150$ K, the temperature of the PdH_x film decreased to 20 K at a cooling rate of 1 K/min to minimize the risk of sample breakage and H desorption. After cooling, H_2 gas was evacuated, and ^3He gas was introduced into the experimental chamber, allowing further cooling for the measurements. The temperature dependence of the resistivity of the PdH_x film obtained using this procedure is shown in Fig. 2(a). The H concentration is estimated to be $x = 0.865$, based on the superconducting transition temperature.

The H reabsorption was performed as follows. After the resistivity measurements in $\text{PdH}_{0.865}$ film shown in Fig. 2(a), the temperature was increased to 150 K. Then, H_2 gas at ~ 0.27 MPa, higher than that used for the absorption at $x = 0.865$, was introduced in the chamber to reabsorb H atoms into the film. After reabsorption was completed, the temperature was lowered again for the resistivity measurements. The results are plotted at $x = 0.870$, which is estimated from the transition temperature $T_{c1} = 2.31$ K. This procedure was repeated to change the H concentration. For H desorption, the temperature was raised to 180 K, and the resistivity was measured. The results are plotted at $x = 0.834$, where the second transition is not visible. Afterward, the H concentration increased again upon loading H atoms at 150 K. The results are plotted at $x = 0.855$.

D. Resistivity in 10- μm wide film

To clarify whether the second transition at T_{c2} originates from H deficiency, we performed resistivity measurements using a Pd film with a width of 10 μm , which is one-tenth smaller than that used in the measurements in Figs. 2(a) and 2(b). The thickness and distance between the two voltage electrodes are 100 nm and 300 μm , respectively. The arrangement of the Au electrodes is the same as that in Fig. A-1(a).

The temperature dependence of the resistivity is plotted in Fig. A-3, where the H absorption is performed at $T = 150$ K. The resistivity decreases sharply below $T_{c1} = 1.70$ K, and

the transition finishes at 1.62 K. The H concentration is $x = 0.850$ at $T_{c1} = 1.70$ K. As in the case of the PdH_{*x*} film with a width of 100 μm , a large residual resistivity remains, which decreases gradually with decreasing the temperature, as shown in the inset. Moreover, the resistivity drops steeply at $T_{c2} = 0.83$ K, leading to zero resistivity. These features agree well with the results in the Pd film with the width of 100 μm shown in Figs. 2(a) and 2(b). Meanwhile, T_{c2} appears at a higher temperature compared to the results for the 100- μm width, although T_{c1} is markedly lowered. This suggests that the transition temperature T_{c2} is independent of T_{c1} .

E. Resistivity in Pd film with Cu electrodes

The Au electrode can form an impurity phase [27, 28], which may affect the superconducting transition of the Pd film. To examine this possibility, we measured the resistivity of the PdH_{*x*} film with Cu electrodes deposited on the Pd film, as illustrated in Fig. A-1(b). The electrodes were not covered with the Pd film.

The results are presented in Fig.A-4, where H absorption was performed at $T = 150$ K in the same manner as for the Au electrodes. These qualitative features are consistent with the results obtained using Au electrodes. As the temperature decreases, the resistivity in the normal state decreases sharply at $T_{c1} = 2.30$ K owing to the superconducting transition. Notably, although the residual resistivity below T_{c1} is considerably smaller than that observed with the Au electrodes, it still remains after the transition, which is followed by the second transition at $T_{c2} = 0.71$ K. The H concentration is estimated to be $x = 0.870$. These results indicate that the emergence of the residual resistivity and the second transition are not due to the influence of the Au electrodes but are instead intrinsic features of superconducting PdH_{*x*}.

-
- [1] T. Fukai, *The Metal-Hydrogen System*, 2nd Edition (Springer, Berlin, 2005).
 - [2] G. Nelin and K. Scöld, *J. Phys. Chem. Solids* **36**, 1175 (1975).
 - [3] R. R. Arons, H. G. Bohn, and H. Lütgemeier, *Solid State Commun.* **14**, 1203 (1974).
 - [4] R. R. Arons, Y. Tamminga, and G. de Vries, *Phys. Stat. Sol.* **40**, 107 (1970).
 - [5] J. Kondo, *Physica B* **125**, 279 (1984).

- [6] J. Kondo, *Physica B* **126**, 377 (1984).
- [7] V. G. Storchak and N. V. Prokof'ev, *Rev. Mod. Phys.* **70**, 929 (1998), and references therein.
- [8] Yu. Kagan and N. V. Prokof'ev, *Phys. Lett. A* **159**, 289 (1991).
- [9] M. Matsumoto and Y. Ohashi, *J. Phys. Soc. Jpn.* **62**, 2088 (1993).
- [10] Y. Ohashi and M. Matsumoto, *J. Phys. Soc. Jpn.* **62**, 3532 (1993).
- [11] T. Regelmann, L. Schimmele, and A. Seeger, *Z. Phys. B* **93**, 303 (1994).
- [12] T. Regelmann, L. Schimmele, and A. Seeger, *Z. Phys. B* **95**, 441 (1994).
- [13] T. Regelmann, L. Schimmele, and A. Seeger, *Hyperfine Interactions*, **105**, 219 (1997).
- [14] R. Kadono, R. F. Kiefl, J. A. Chakhalian, S. R. Dunsiger, B. Hitti, W. A. MacFarlane, J. Major, L. Schimmele, M. Matsumoto, and Y. Ohashi, *Phys. Rev. Lett.* **79**, 107 (1997).
- [15] T. Skoskiewicz, *Phys. Status Solidi A* **11**, K123 (1972).
- [16] T. Kawae, Y. Inagaki, S. Wen, S. Hirota, D. Itou, and T. Kimura, *J. Phys. Soc. Jpn.* **89**, 051004 (2020), and references therein.
- [17] R. W. Standley, M. Steinback, and C. B. Satterthwaite, *Solid State Commun.* **31**, 801 (1979).
- [18] R. J. Miller and C. B. Satterthwaite, *Phys. Rev. Lett.* **34**, 144 (1975).
- [19] H. Hemmes, A. Driessen, R. Griessen, and M. Gupta, *Phys. Rev. B* **39**, 4110 (1989).
- [20] A. P. Drozdov, M. I. Eremets, I. A. Troyan, V. Ksenofontov, and S. I. Shylin, *Nature* **525**, 73 (2015).
- [21] M. Somayazulu, M. Ahart, A. K. Mishra, Z. M. Geballe, M. Baldini, Y. Meng, V. V. Struzhkin, and R. J. Hemley, *Phys. Rev. Lett.* **122**, 027001 (2019).
- [22] A. Drozdov, P. Kong, V. Minkov, S. Besedin, M. Kuzovnikov, S. Mozaffari, L. Balicas, F. Balakirev, D. Graf, V. Prakapenka, E. Greenberg, D. A. Knyazev, M. Tkacz, and M. I. Eremets, *Nature* **569**, 528 (2019).
- [23] Y. Inagaki, S. Wen, Y. Kawasaki, H. Takata, Y. Furukawa, and T. Kawae, *J. Phys. Soc. Jpn.* **87**, 123701 (2018).
- [24] R. Kato, R. Koga, K. Miyakawa, M. Shiga, Y. Inagaki, and T. Kawae, *JPS Conf. Proc.* **38**, 011033 (2023).
- [25] R. Kato, T. Yoshida, R. Iimori, Tai Zizhou, M. Shiga, Y. Inagaki, T. Kimura, and T. Kawae, *J. Phys. Soc. Jpn.* **93**, 024703 (2024).
- [26] Y. Sato, S. Makiyama, Y. Sakamoto, T. Hasuo, Y. Inagaki, T. Fujiwara, H. S. Suzuki, K. Matsubayashi, Y. Uwatoko, and T. Kawae, *Jpn. J. Appl. Phys.* **52**, 106702 (2013).

- [27] R. J. Smith and D. A. Otterson, *J. Phys. Chem. Solids*, **31**, 187 (1970).
- [28] T. B. Flanagan and D. Wang, *J. Phys. Chem. C* **115**, 11618 (2011).
- [29] K. Namba, S. Ogura, S. Ohno, Wen Di, K. Kato, M. Wilde, I. Pletikosi, P. Pervan, M. Milun, and K. Fukutani, *Proc. Natl. Acad. Sci.* **115**, 7896 (2018).
- [30] I. F. Silvera and J. T. M. Walraven, *Progress in Low Temperature Physics*, Vol. **10**, 139 (1986).
- [31] G. B. Blatter, M. V. Feigelman, V. Geshkenbein, A. I. Larkin, V. M. Vinokur, *Rev. Mod. Phys.* **66**, 1125 (1994).
- [32] A. M. Petrean and L. M. Paulius, W.-K. Kwok, J. A. Fendrich, and G.W. Crabtree, *Phys. Rev. Lett.* **84**, 5852 (2000).
- [33] M. Liao, H. Wang, Y. Zhu, R. Shang, M. Rafique, L. Yang, H. Zhang, D. Zhang, and Q.-K. Xue, *Nat. Commun.* **12**, 5342 (2021).
- [34] A. O. Caldeira and A. J. Leggett, *Ann. Phys. (N.Y.)* **149**, 374 (1983).
- [35] H. Grabert and U. Weiss, *Phys. Rev. Lett.* **54**, 1065 (1985).
- [36] H. Akiba, H. Kobayashi, H. Kitagawa, M. Kofu, and O. Yamamuro, *Phys. Rev. B* **92**, 064202 (2015).
- [37] A. S. Oya and O. V. Lounasmaa, *Rev. Mod. Phys.* **69**, 1 (1997).
- [38] R. Wisniewski and A. J. Bostocki, *Phys. Rev. B* **3**, 251 (1971).
- [39] B. Baranowski and R. Wiśniewski, *Phys. Status Solidi* **35**, 593 (1969).

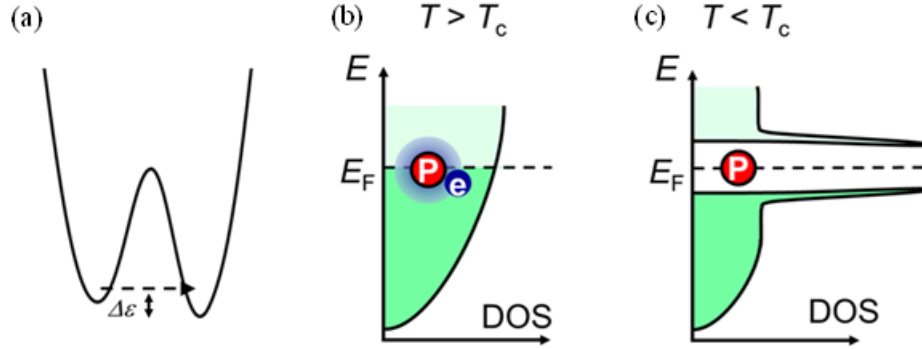


FIG. 1: Schematic illustration of hydrogen tunneling absorbed in a normal metal and a superconductor. (a) A schematic illustration of tunneling. Hydrogen can traverse an energy barrier between two interstitial sites, where $\Delta\varepsilon$ is the potential difference of the two wells. (b) In a normal metal, the electron density around the H atom increases due to the positive charge of the proton. Consequently, the tunneling proton migrates, dragging the electron cloud in diffusion. (c) In a superconductor, the emergence of an energy gap on the Fermi surface significantly reduces the interaction between the proton and conduction electrons, thereby enhancing the tunneling probability of proton during diffusion.

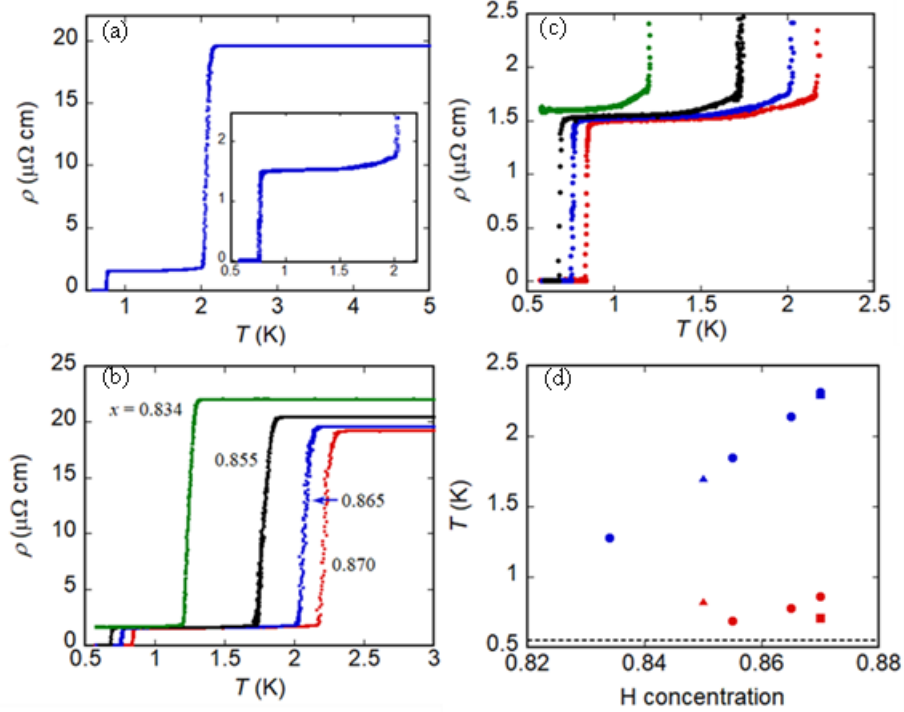


FIG. 2: Temperature dependence of the resistivity in PdH_x films. (a) Temperature dependence of resistivity of the PdH_x film, in which H atoms were absorbed at $T = 150$ K. The superconducting transition occurs at $T_{c1} = 2.14$ K, from which the H concentration is estimated to be $x = 0.865$. The inset shows the low-temperature behavior. The resistivity drops steeply at $T_{c2} = 0.78$ K, resulting in zero resistivity. (b) Temperature dependence of resistivity at $x = 0.870$, 0.865 , 0.855 , and 0.834 , which correspond to the curves at $T = 3$ K from the bottom to top. The H concentration is varied by changing the absorption temperature, as described in Fig. A-2. (c) Enlarged view of the low-temperature region in (b). (d) H-concentration dependence of T_{c1} and T_{c2} , marked by blue and red color, respectively. Circle, triangle, and square represent the transition temperatures in the Pd film depicted in (b), Pd film with a width of $10 \mu\text{m}$ in Fig. A-3 and Pd film with Cu electrodes in Fig. A-4, respectively. The dotted line indicates the minimum temperature in the measurements.

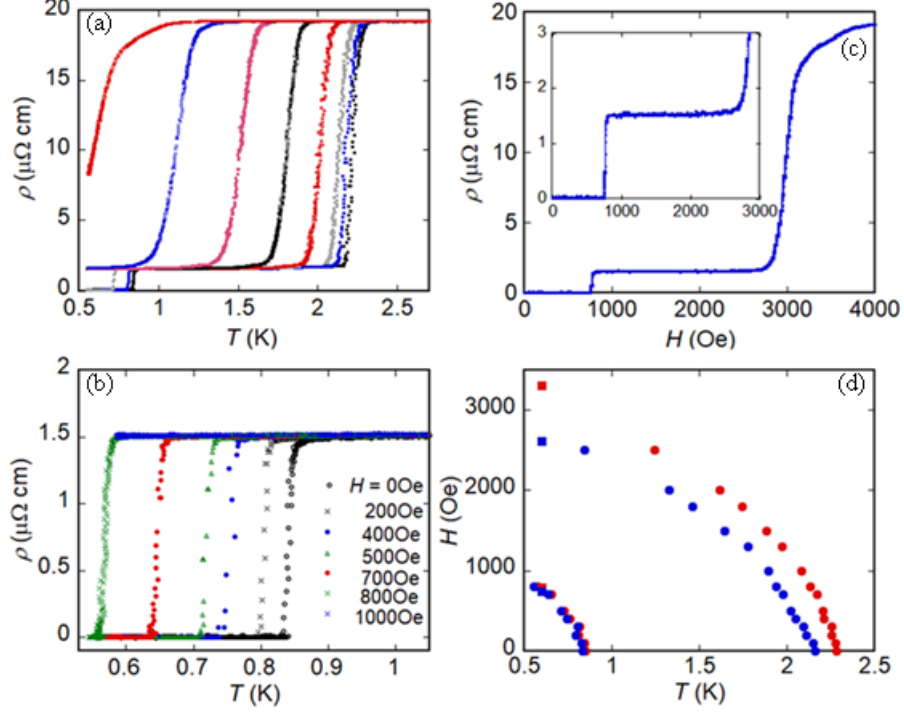


FIG. 3: Magnetic field dependence of the resistivity in PdH_x film. (a) Temperature dependence of the resistivity in PdH_{0.870} film at $H = 0$ Oe, 300 Oe, 500 Oe, 1000 Oe, 1500 Oe, 2000 Oe, 2500 Oe, and 3000 Oe. The transition curve at T_{c1} is broadened with increasing the magnetic field. (b) Temperature dependence of the resistivity at $H = 0$ Oe, 200 Oe, 400 Oe, 500 Oe, 700 Oe, 800, and 1000 Oe in the low temperature region. The step drop of the resistivity is observed up to $H = 800$ Oe. (c) Magnetic field dependence of the resistivity at $T = 0.6$ K. The resistivity increases steeply at around $H = 750$ Oe, followed by almost a constant resistivity up to ~ 2500 Oe, as shown in the inset. Subsequently, it increases sharply at around 2700 Oe. (d) Temperature vs. magnetic field phase diagram of T_{c1} and T_{c2} for PdH_{0.870}. For both transitions, the onset (red circle) and endpoint (blue circle) are defined as 10 % drop point from the normal (residual) resistivity and converging point to the baseline determined by the residual (zero) resistivity, respectively. Red and blue squares are derived from the magnetic dependence of the resistivity at $T = 0.6$ K in (c), with transition points determined similarly.

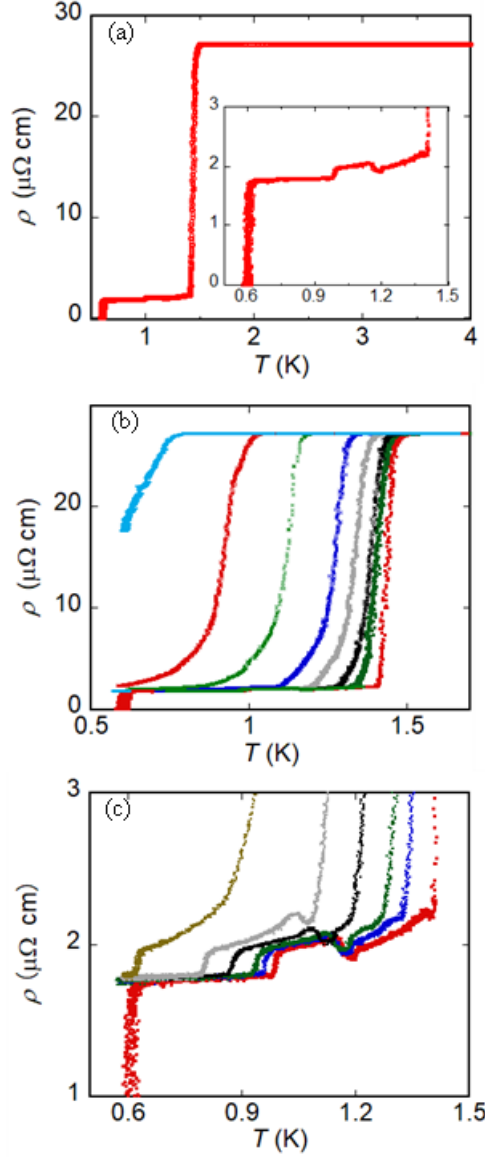


FIG. 4: Temperature dependence of the resistivity in PdD_x film. (a) Temperature dependence of resistivity of the PdD_x film, in which H atoms were absorbed at $T = 170$ K. The superconducting transition occurs at $T_{c1} = 1.47$ K, from which x is estimated to be 0.795. A residual resistivity remains after the superconducting transition and the second transition occurs at $T_{c2} \sim 0.6$ K. Additionally, a rectangular-shaped anomaly appears between $T = 0.95$ K and 1.2 K. (b) Temperature dependence of the resistivity at $H = 0$ Oe, 300 Oe, 500 Oe, 700 Oe, 1000 Oe, 1500 Oe, 2000 Oe, and 3000 Oe in $\text{PdD}_{0.795}$. The sample structure is identical to that used in Figs. 2 and 3. The transition curve at T_{c1} is broadened with increasing the magnetic field, similar to the behavior observed in PdH_x . (c) Low-temperature resistivity as a function of temperature at $H = 0$ Oe, 300 Oe, 500 Oe, 700 Oe, 1000 Oe, and 1500 Oe in the low temperature region. A rectangular-shaped structure between $T = 0.95$ K and 1.2 K shifts to lower temperatures as the magnetic field increases.

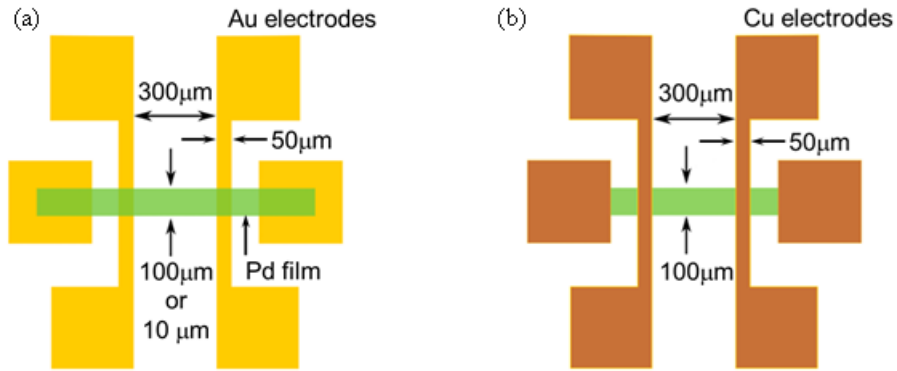


FIG. A-1: Schematic illustration of Pd film. (a) Pd films with Au electrodes having a thickness of 20 nm and a width of $50\mu\text{m}$. The electrodes are prepared on a SiO_2/Si substrate with a 5-nm Ti layer deposited below the Au electrodes. A Pd film with a thickness of 100 nm and a width of 100 or $10\mu\text{m}$ is deposited on the substrate with Au electrodes. The distance between the two voltage electrodes is $300\mu\text{m}$. (b) Pd film with Cu electrodes. After the Pd film with a thickness of 100 nm and width of $100\mu\text{m}$ is deposited on a SiO_2/Si substrate by magnetron sputtering, the electrodes with a thickness of 100 nm and a width of $50\mu\text{m}$ are deposited on the film by thermal evaporation. The distance between the two electrodes is $300\mu\text{m}$.

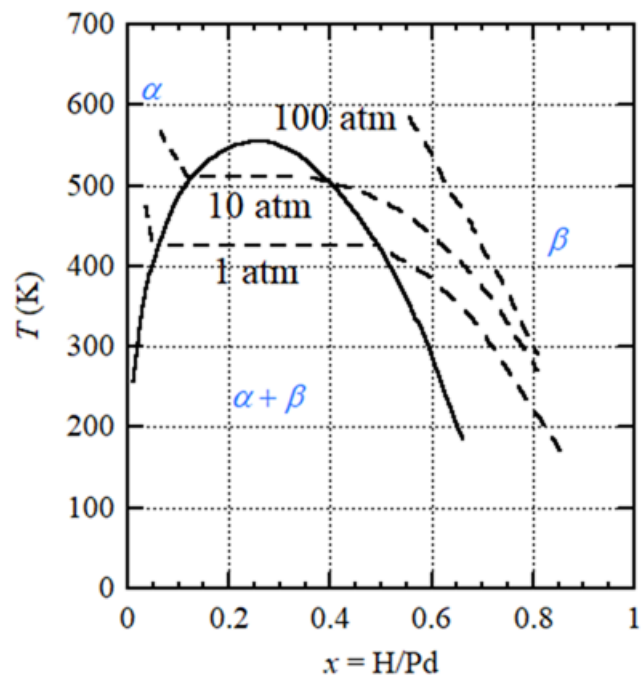


FIG. A-2: The H concentration–pressure–temperature (x – P – T) phase diagram of Pd–H systems. The H concentration in Pd ($x = \text{H/Pd}$) increases with decreasing temperature at the same H pressure.

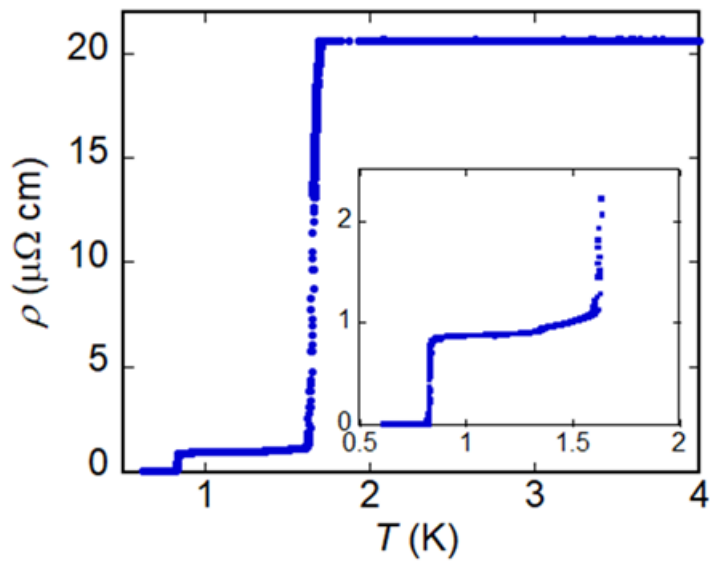


FIG. A-3: Temperature dependence of resistivity in a Pd-hydride film for a small size. Temperature dependence of resistivity of a PdH_x film with a width of $10 \mu\text{m}$ in which H atoms are absorbed at $T = 150$ K. The superconducting transition and second transition occur at $T_{c1} = 1.70$ K and at $T_{c2} = 0.83$ K, respectively. The inset shows the low-temperature behavior.

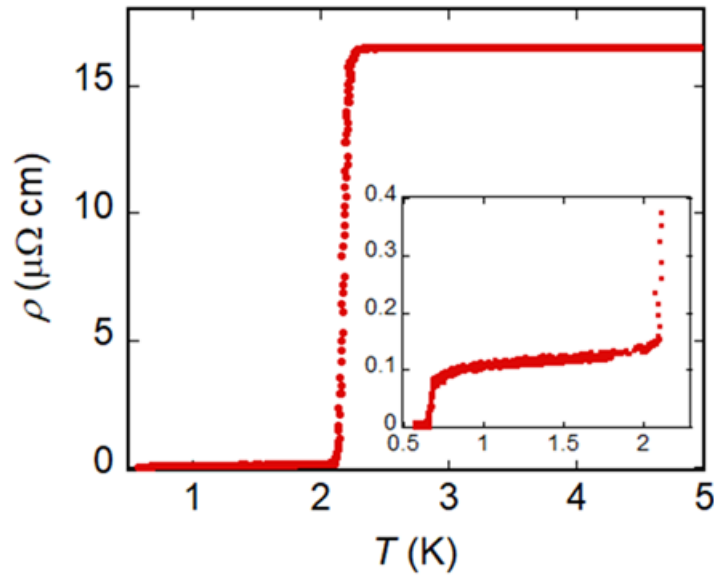


FIG. A-4: Temperature dependence of resistivity in a Pd-hydride film with Cu electrodes. Temperature dependence of resistivity in a Pd film with Cu electrodes, where H atoms are loaded at $T = 150$ K. The superconducting transition occurs at $T_{c1} = 2.30$ K and finishes at 2.15 K. The inset shows the low-temperature behavior. As in the case of the Au electrodes, a residual resistivity remains, and a sharp drop occurs at $T_{c2} = 0.71$ K.